

Chapter 8

Cosmic Rays

8.1 Composition and energy distribution

Cosmic rays can be broadly defined as the massive particles, photons (γ rays, X-rays, ultra-violet and infrared radiation, ...), neutrinos, and exotics (WIMPS, axions,...) striking the earth. The primary cosmic rays are those entering the upper atmosphere, the cosmic rays of the interstellar medium. Secondary cosmic rays are those produced by the interactions of the primary rays in the atmosphere or in the earth. Also products of cosmic ray interactions in the interstellar medium (e.g., spallation products from cosmic ray - cosmic ray collisions) are also labeled as secondary cosmic rays. Cosmic rays can be of either galactic (including solar) or extragalactic origin.

If we confine ourselves to the particle constituents (protons, nuclei, leptons), their motion in the galaxy has been roughly randomized by the galactic magnetic field. (We will mention some exceptions to this below.) Thus they provide very little information about the direction of the source. The peak of the distribution in energy is in the range of 100 MeV - 1 GeV. The intensity of cosmic rays of energy 1 GeV/ nucleon or greater is about $1/\text{cm}^2\text{sec}$. The energy density corresponding to this is thus about $1 \text{ eV}/\text{cm}^3$. This can be compared to the energy density of stellar light of $0.3 \text{ eV}/\text{cm}^3$.

The chemical composition of (primary) cosmic rays is shown in the figure. This distribution is approximately independent of energy, at least over the dominant energy range of 10 MeV/nucleon through several GeV/nucleon. About 90% of nuclear cosmic rays are protons, about 9% He nuclei, and 1% heavier nuclei. The composition has been measured by instruments mounted on balloons, satellites, and spacecraft. The figure also shows the chemical distribution of the elements in our solar system, which differs from that of the cosmic rays in some remarkable ways. The most dramatic of these is an enormous enrichment in the

cosmic rays of the elements Li/Be/B. Note also that there is enrichment in even Z elements relative to odd Z , when normalized to solar system abundances. Finally the cosmic rays are relatively enriched in the heaviest elements relative to H and He.

Although not shown in the figure, many elements heavier than the iron group have been measured with typical abundances of 10^{-5} of iron. Much of this information was gained from satellite and spacecraft measurements over the last decade. Some of the conclusions:

- 1) Abundances of even Z elements with $30 \lesssim Z \lesssim 60$ are in reasonable agreement with solar system abundances.
- 2) In the region $62 \lesssim Z \lesssim 80$, which includes the platinum-lead region, abundances are enhanced relative to solar by about a factor of two. This suggests an enhancement in r-process elements, which dominate this mass region.

There are obvious connections between other astrophysics we have discussed (e.g., if the r-process site is core-collapse supernovae, then one would expect enrichment in r-process nuclei as supernovae are also believed to be the primary acceleration mechanism for lower energy cosmic rays) and possible deviations from solar abundances in the cosmic rays.

Galactic cosmic rays are fully ionized: the acceleration mechanisms fully strip the ions. Cosmic rays also have an antimatter component, as measured in the Space Shuttle Discovery AMS (Alpha Magnetic Spectrometer) experiment. The AMS detected about 200 antiprotons above 1 GeV, generally attributed to nuclear collisions of CR particles with interstellar matter.

The energy distribution of cosmic rays from about 10^{10} eV to about 10^{15} eV has a power-law distribution

$$\text{particles/cm}^2\text{secMeV/n} \propto E^{-s}$$

with s between -1.6 and -1.7. However there is a break or “knee” in the curve at about 10^{15}

Table 2.1: Relative and absolute CR abundance ($E > 2.5\text{GeV/nuc}$, [?])

particle group	nucleus charge	integral particle intensity $m^{-2} s^{-1} sr^{-1}$	number of particles per 10^5 protons	
			in CR	in the Universe
protons	1	1300	10000	10000
helium	2	94	720	1600
L	3-5	2	15	10^{-4}
M	6-9	6.7	52	14
H	10-19	2	15	6
VH	20-30	0.5	4	0.06
SH	> 30	10^{-4}	10^{-3}	$7 \cdot 10^{-5}$
electrons	1	13	100	10000
antiprotons	1	> 0.1	5	???

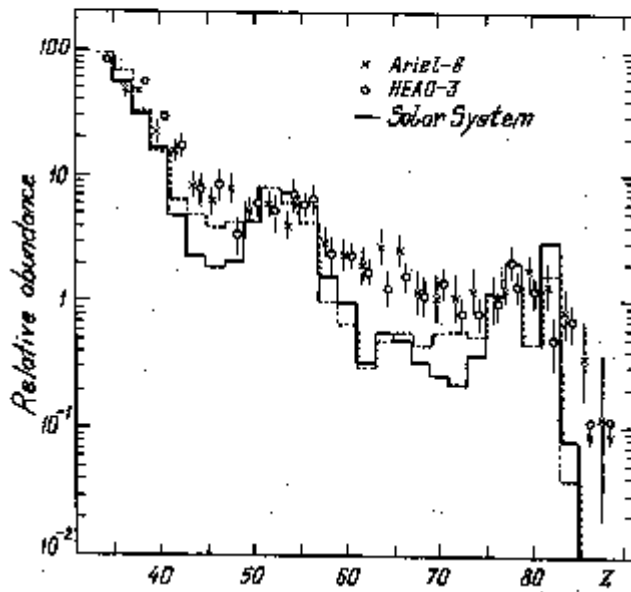
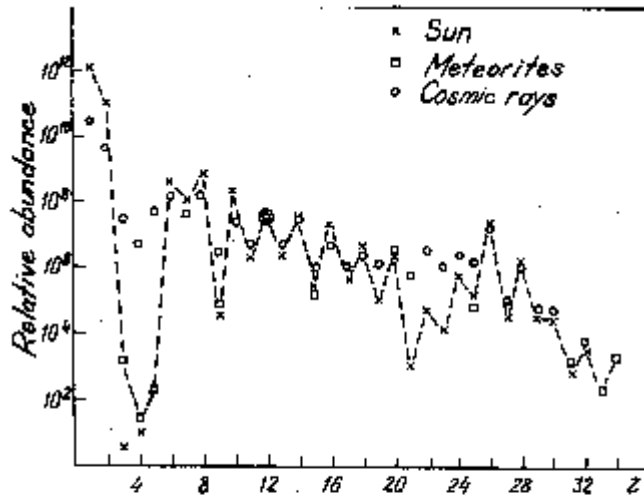


Figure 2.1: Relative abundance of elements in cosmic rays and in the solar system.

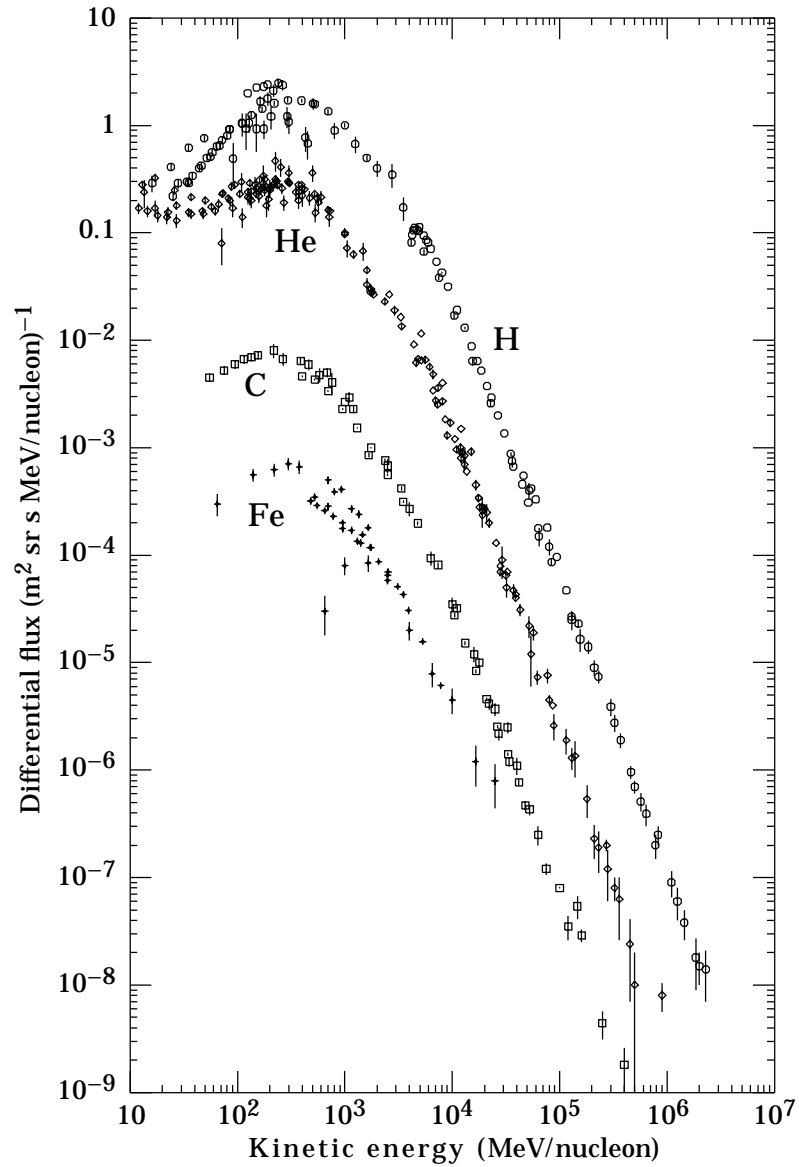


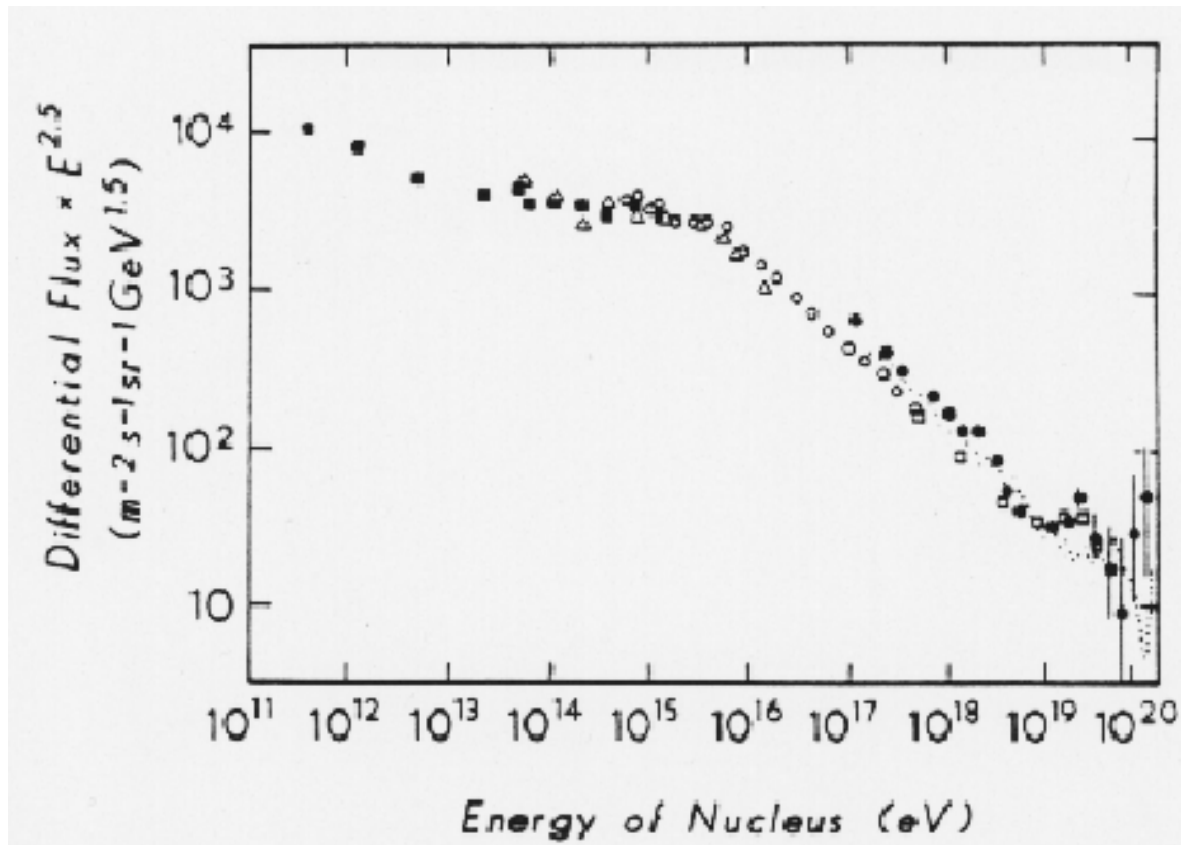
Figure 20.1: Major components of the primary cosmic radiation (from Ref. 1).

eV. The slope sharpens above this knee (see the figure), falling with s ranging from -2.0 to -2.2, eventually steeping to an exponent of above -2.7. The knee is generally attributed to the fact that supernovae acceleration of cosmic rays is limited to about this energy. This would argue that the cosmic rays above this energy either have a different origin, or were further accelerated after production. Sometimes this break is associated with the inability of supernova shocks to accelerate particles to energies beyond the knee. However the sharpness of the knee has troubled many of the experts: it is very difficult to find natural models producing such a defined break.

8.2 Propagation and origin

The most common toy model for galactic cosmic rays is called the "leaky box" model. It assumes that the cosmic rays are confined within the galactic disk, where the mass density is high, but with some gradual leaking out of the disk. This model does a good job in explaining the energy-dependence of the life of cosmic rays (more on this later). But others have argued for other models, including closed models where cosmic rays are fully confined, then explaining lifetimes through devices such as a combination of a few nearby and many distant cosmic ray sources.

The conventional explanation for the most dramatic isotopic anomaly in the cosmic ray, the enrichment in Li/Be/B by about six orders of magnitude, is that they are produced in the interstellar medium when accelerated protons collide with C, N, and O. We discussed this process earlier. The enrichment of odd-A nuclei (these also tend to be relatively rare in their solar distribution since stellar processes tend to favor production of more stable even-A nuclei) is usually also attributed to spallation reactions off more abundant even-A nuclei. These associations immediately lead to some interesting physics conclusions because, from the known density of cosmic rays (at least in the earth's vicinity) and from known spallation cross sections, one can estimate the amount of material through which a typical cosmic ray propagates. Although the estimates are model dependent - and probably not sufficiently



interesting to go through in detail - typical values are 4 - 6 g/cm² for the effective thickness. Now the mass density within intragalactic space is about 1 proton/cm³, or about 1.7 · 10⁻²⁴ g/cm³. Thus taking a velocity of c, we can crudely estimate the cosmic ray lifetime

$$1.7 \times 10^{-24} \text{g/cm}^3 \times (3 \cdot 10^{10} \text{cm/sec}) \times t = (4 - 6) \text{g/cm}^2$$

So this gives

$$t \sim 3 \cdot 10^6 \text{y}$$

This calculation assumes an average galactic mass density that is not known by direct measurement. Thus it is nice that a more direct estimate of the galactic cosmic ray lifetime is provided by cosmic ray radioactive isotopes. The right chronometer is one that has a lifetime in the ballpark of the estimate above. ¹⁰Be, with a lifetime of 1.51 · 10⁶ y, is thus quite suitable. It is a cosmic ray spallation product: this guarantees that it is born as a cosmic ray. Its abundance can be normalized to those of the other, stable Li/Be/B isotopes: the spallation cross sections are known. Thus the absence of ¹⁰Be in the cosmic ray spectrum would indicate that the typical cosmic ray lifetime is much larger than 1.51 · 10⁶ y. The survival probability should also depend on the ¹⁰Be energy, due to time dilation effects. One observes a reduction in ¹⁰Be to about (0.2-0.3) of its expected instantaneous production, relative to other Li/Be/B isotopes. From this one concludes

$$t \sim (2 - 3) \cdot 10^7 \text{years}$$

This suggests that the mass density estimate used above (in our first calculation) may have been too high by a factor of 5-10.

In modeling the origin of cosmic rays, the first conclusion, given their richness in metals, is that must come from highly evolved stars such as those that undergo supernovae. We have already noted the abundance of r-process nuclei, which could be taken as a “smoking gun” of supernova dominance, for those who accept that supernovae are the r-process site.

However this is clearly not the full picture. Studies of the isotopic composition as the knee is approached shows that the composition changes: the spectrum of protons becomes noticeably steeper in energy, while the iron group elements do not show such a dramatic change. Above the knee - at energies above 10^{16} eV the galactic magnetic field is too weak to appreciably trap particles. Thus it is probable that at these high energies the character of the cosmic rays changes from primarily galactic to primarily extragalactic. This also suggests a natural explanation for the relative enrichment in heavy nuclei in the vicinity of the knee: the upper energy of confined particles should vary as Z , since the cyclotron frequency for particles of the same velocity varies as $Z \times B$. Above 10^{18} eV/n the cosmic rays free stream through galaxies.

The cosmic rays appear to be approximately isotropic – once one gets above about 50 GeV to escape local magnetic effects. An exception is a small anisotropy measured by AGASA, excess events at about 10^{18} eV pointing back to the galactic center. An interesting speculation is that these are neutrons, which because of time dilation can reach the solar system once they reach 10^{18} eV. If this result is true, it would argue for a central galactic accelerator that (most likely) is capable of accelerating ions up to 10^{18} eV per nucleon.

8.3 The highest energy cosmic rays and the GZK cutoff

Some of the most curious observations in cosmic ray physics have to do with the highest energy cosmic rays. A number of new instruments, such as the Fly's Eye, the Pierre Auger, and the AGASA detectors, are designed with sensitivity to ultrahighenergy cosmic rays. For example, the Fly's Eye uses air fluorescence to detect UHE cosmic rays. An extensive air shower is generated when a primary cosmic ray interacts with the atmosphere. This is imaged using the fluorescence light produced by excitation of the nitrogen molecules by the secondaries in the extensive air shower. The shape of the shower allows the experimenters to reconstruct the energy of the primary. It also may provide some information on composition. The Fly's Eye can provide stereo information on the developing shower because of detector

arrays located 3.4 km apart.

The rare high energy events show some structure, particularly around 10^{19} eV, where the spectrum flattens from a slope of about -3.0 to one of about -2.6. Furthermore, both of the major groups have seen events above the Greisen-Zatsepin-Kuzmin cutoff of about 10^{20} eV. I believe there are now tens of such events extending up to about 10^{22} eV.

The cosmic medium is filled by background radiation of relic photons, left over from the back bang and noninteracting since the time electrons and nuclei recombined to form atoms. Their typical energy is about 10^{-3} eV. We consider the propagation of a high energy proton through this medium.

Let $p_\mu = (\epsilon, \vec{p})$ be the photon four-momentum. Then $|\vec{p}| = \epsilon$. Let $P_\mu = (\omega, \vec{P})$ be the proton four-momentum. We evaluate in the center-of-mass

$$(P^\mu + p^\mu)(P_\mu + p_\mu) = (\omega + \epsilon)^2 = \epsilon_{CM}^2$$

which we recognize as the square of the center-of-mass energy. Note that if ϵ_{CM} exceeds

$$m_\pi + M_N$$

then clearly the reaction

$$\gamma + N \rightarrow \pi + N$$

can occur, degrading the nucleon energy. But the center-of-mass energy is a Lorentz invariant quantity, so it can be evaluated in the laboratory frame

$$\epsilon_{CM}^2 = M_N^2 + \omega\epsilon - \vec{P} \cdot \vec{p}$$

As the cosmic background photons are moving in all directions, we are free to maximize the RHS by taking $\cos\theta \sim -1$. Noting that the incident nucleon is highly relativistic

$$(\epsilon_{CM}^{max})^2 \sim M_N^2 + 2\omega\epsilon$$

Thus the requirement for photoproduction is $\epsilon_{CM}^{max} \gtrsim m_\pi + M_N \Rightarrow$

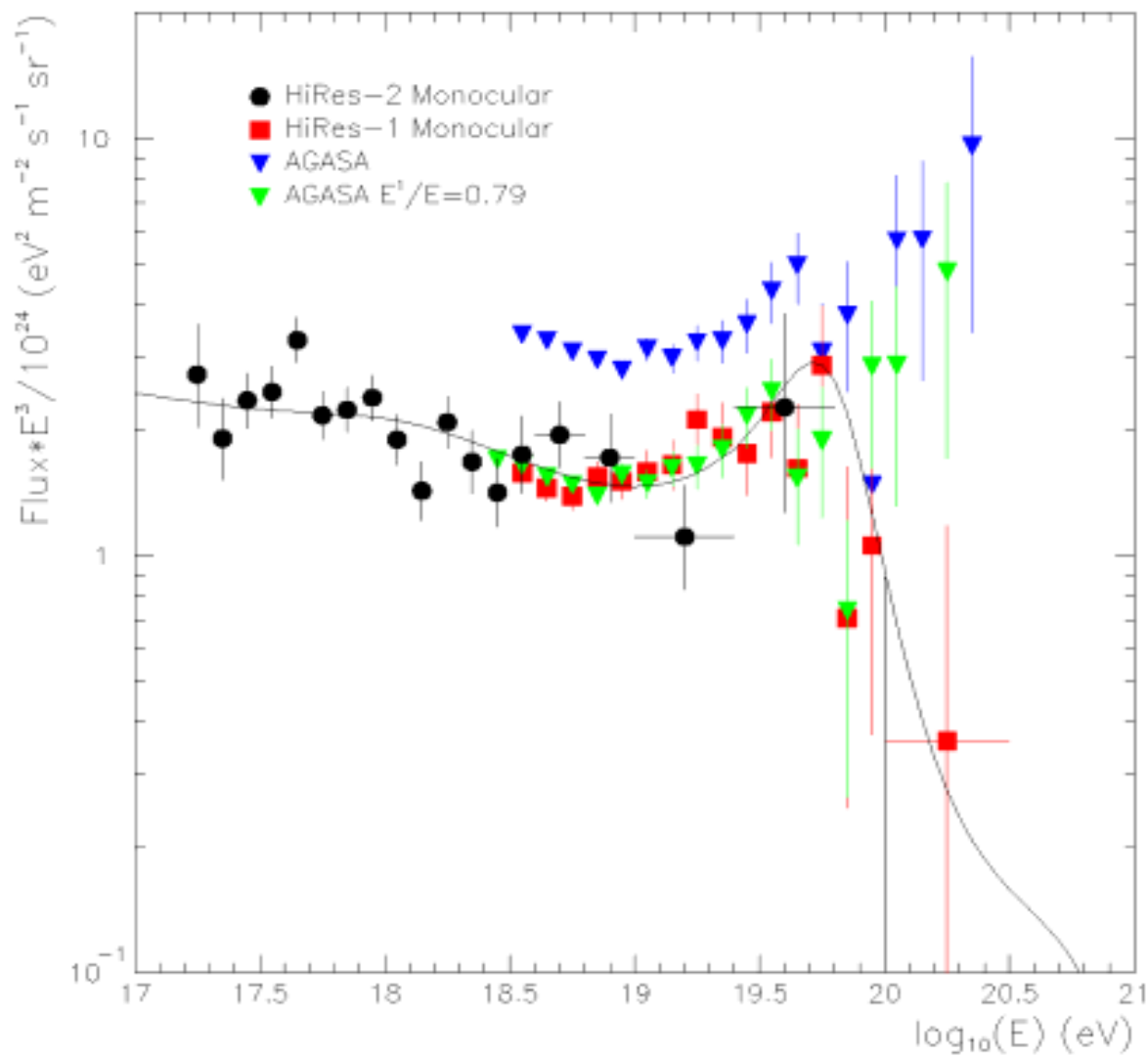
$$\omega \gtrsim \frac{m_\pi^2 + 2M_N m_\pi}{2\epsilon}$$

$$\sim 1.4 \cdot 10^{20} \text{ eV}$$

This results in a mean free path for protons of about 10^8 light years for protons at $\sim 10^{20}$ eV or higher energies, a distance substantially smaller than the horizon. Thus if the origin of such cosmic rays is all of extragalactic space, there should be a very sharp cutoff in the cosmic ray flux at about this energy. This is called the Greisen-Zatsepin-Kuzmin cutoff, and is shown in the figure. Yet the very high energy events from AGASA show no evidence for any such cutoff.

There are some disagreements among groups about how well energies are reconstructed. But if the results are correct, it is an interesting puzzle. Fairly mundane solutions have been offered, such that these high energy events are exclusively nuclear (CNO elements and then iron), which can achieve higher energies at lower velocities. It has been suggested that the events are secondaries from the collisions of still higher energy neutrinos. However this requires new physics in that the Standard Model predicts a declining neutrino cross section above the Z mass that would not be sufficient to produce the needed event rate, it is thought. It could be that ultrahigh energy cosmic rays both above and below the GZK cutoff are of relatively local origin. That would avoid the puzzle; but it would raise a new question of what confines the cosmic rays if they are extragalactic but somehow produced primarily in a local region about us. Perhaps we are somehow near some remarkable local source or sources: our position in the cosmos is special. All of this is intriguing.

The nuclear solution does not evade all of the problems as other types of GZK cutoffs effect nuclear species. At a center-of-mass energy considerably lower nuclei can absorb (in their



rest frame) a photon of energy ~ 10 MeV, resulting in photodisintegration. This leads to a GZK cutoff for iron nuclei of

$$\sim 10^{19} \text{eV}$$

. An issue related to this that I have not seen discussed is the slowing down of nuclei due to absorption and reradiation of cosmic background photons. Perhaps typical cross sections for photoabsorption are too small for this effect to be of interest. But I would think this conclusion could depend on whether the ultra-high-energy cosmic ray acceleration mechanism is gradual or not: if very gradual, perhaps this photoabsorption viscosity could be interesting for nuclei with strong, low-lying excitations.

8.4 Gamma rays

The properties of the earth's atmosphere divides gamma ray astronomy into two halves. From the ultraviolet to gamma rays of energy ~ 20 GeV the atmosphere is opaque. Thus observations in this energy range must be done with instruments mounted in satellites or carried by balloons. The ease of detecting the radiation generally goes up with energy, but the strengths of typical astrophysical sources go down. The net result is that one can do a lot over this range: this motivated the design of the four instruments on board the Gamma Ray Observatory. For gamma rays above 20 GeV, interactions in the atmosphere produce showers that can be observed either by the Cerenkov light produced by the secondaries or, at high altitude, by direct detection of the secondaries. Of course, observations can also be (and are) made by space-bound detectors, too.

Many of the concerns of this field are driven by instrumental issues (so it would be better to have an experimentalist giving this talk). The central issues are rather obvious:

- Producing detectors with greater sensitivity. The dynamic range of existing detectors - the gap between the brightest nearby sources such as the Crab and the faintest detectable sources - is typically about a factor of 100. Thus the situation is equivalent to being able to

see no stars fainter than the 5th magnitude. Improvements in sensitivity can thus greatly extend the horizon of our observations, while also allowing much more detailed spectral studies of known bright sources. Greater sensitivity can be achieved with great collection areas and by reducing ambient backgrounds. The push towards greater size is clearly an expensive challenge given the necessity for observing outside the atmosphere.

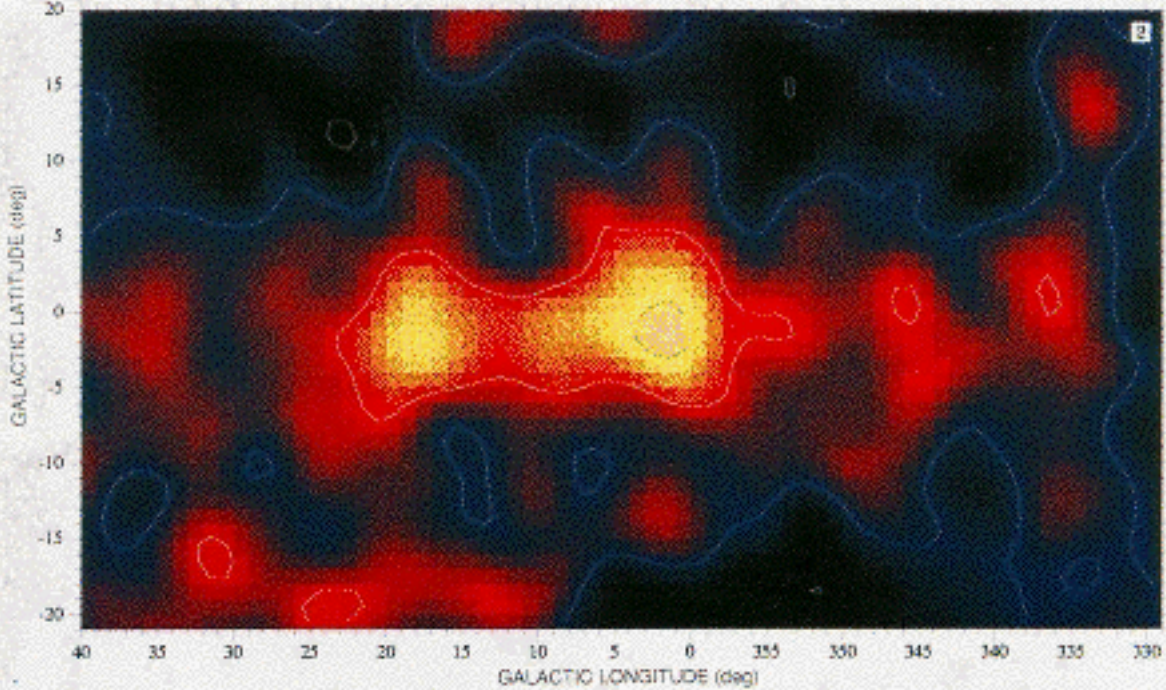
- Enhancing spectral resolution. This includes both enhanced spectral resolution and enhanced spatial resolution, the latter required to better identify sources.
- Enhanced temporal covering and resolution.

Examples of why such extended capabilities are important are provided by the GRO instruments. For example, BATSE - the Burst and Transient Source Experiment - was designed as an all-sky monitor with sharp timing capability. This proved decisive in demonstrating that gamma ray bursts are distributed approximately isotropically. This detector also led to the discovery of new pulsars, x-ray novae, and the identification of one soft gamma ray repeater. Likewise another GRO instrument EGRET - the Energetic Gamma Ray Experiment - was able to correlate high energy gammas with the lower energy bursts detected by BATSE. It also measured high energy gammas from active galaxies.

8.5 Nuclear Gamma Rays

We have touched on this theme before, but here I'd like to gather together several examples of what is becoming possible. One of these examples is ^{26}Al , which has a 720,000 y lifetime for decay to ^{26}Mg . The decay of the 5^+ ground state populates the first two excited states of ^{26}Mg , which are 2^+ states with energies of 2.938 and 1.809 MeV. The latter state is populated 97% of the time, so the primary signature is a 1.809 MeV γ . The 2.938 MeV state decays to the 1.809 MeV level, so a small number of 1.129 MeV γ s are also produced.

The primary site for producing ^{26}Al is thought to be Type II and IIb supernovae. Additional aluminum may come from the winds of very massive stars. COMPTEL has produced



a galactic map of the 1.809 MeV γ s. That map differs from higher energy (~ 100 MeV) maps in that there is marked clumpiness to the production, including intense sources associated with Cygnus, Vela, etc. This map is interpreted as an indicator of recent supernova activity. The conclusions drawn from such a map are clearly model dependent because one obtains an angular distribution but no spatial depth information. But under the assumption that the entire galaxy is contributing in the expected way, one deduces a recent supernova rate of 3.4 ± 2.8 /century. The model dependence also includes the uncertainty in the aluminum production per event. The attribution of the total flux to the Al injection rate of massive stars yields an upper bound on the recent star formation rate of $5 \pm 4 M_{\odot}$ per year. This calculation, of course, requires not only a model of the Al production per supernova, but also a model of the range of stellar masses that undergo core collapse and a model for the distribution of stars with mass (populations roughly decline exponentially with an exponent of about -2.35).

In a similar way, ^{44}Ti decay proceeds with a ~ 60 year half life to the ground state of ^{44}Sc , which in turn electron captures to ^{44}Ca . The order of the states in Sc is 2^+ (gs), 1^- (68 keV), and 0^- (146 keV). The decay feeds the second excited state 98% of the time, which then decays through the 1^- state to the ground state, producing γ s of 78 and 68 keV. The subsequent decay to ^{44}Ca has a 4 hour lifetime and produces a 1.157 MeV γ , as the 2^+ first excited state of ^{44}Ca is populated 99% of the time. The ~ 100 keV line for the the source Cas A is within the detection abilities of OSSE, while the 1.157 MeV line can be seen by COMPTEL.

Various types of supernovae are thought to produce ^{44}Ti , including both types I and II. As in the case of the ^{26}Al line, the galaxy is effectively transparent to the produced γ ray, so the detection provides a measure of the very recent supernova rate free from worries about obscuration. One expects to have a sensitivity with COMPTEL to nearby supernovae occurring within the past 1000 years, or 15 half lives. Given a supernova rate of some several per

century, it is clear that the distribution should be from quite localized sources, representing recent events. Typical productions of ^{44}Ti from supernovae are, according to modelers, on the order of $10^{-4} M_{\odot}$ per event.

The youngest known galactic supernova remnant is Cas A, noted optically by John Flamsteed in 1680. COMPTEL reported the observation of ^{44}Ti γ s from Cas A in 1994. The very recent report of a survey extending over a six-year period beginning in 1991 found only one additional source, identified with a young supernova remnant not observed either optically or in the radio. The source is located in the direction of the Vela constellation. Constraints on the doppler broadening of the 1.16 MeV line limits the velocity of the ejecta to no more than 19000 km/sec. The COMPTEL results are confirmed by ROSAT xray data of the vela region, which found a shell-type supernova remnant at the same location. The shell temperature is on the order of several keV, which also indicates a young remnant. Finally, COMPTEL previously saw ^{26}Al in this region, attributing this to the known Vela supernova remnant. However the centroid of that distribution has been argued to better fit the new supernova remnant. Modelers are currently engaged in arguments about the nature of the progenitor, using both the ejection velocity bound and the ^{44}Ti yield to bound models. One possibility is a core-collapse supernova of a massive star that had previously lost its hydrogen envelope. It has been claimed that a supernova at this distance (100-300 pc, derived from the Ti γ flux and age estimates of 600-1100 years based on the expansion velocity) could have been as bright as the moon, leaving an interesting question as to why it was not observed.

Finally, there have been recent papers suggesting that future generations of gamma ray detectors might see γ s in the energy range of 100-700 keV associated with elements specific to the r-process. Establishing a correlation between such γ s and known supernova remnants could thus establish the r-process site and, potential, constrain the total r-process production per site. One of the candidates, ^{126}Sb , has a 144,000 year lifetime, easily long enough

to allow a galaxy survey. It produces lines at 415, 666, and 695 keV. The proposed detector ATHENA possibly could detect ^{126}Sb lines from Vela.

8.6 Astrophysics of High Energy Gammas

EGRET succeeded in identifying on the order of 100 high-energy gamma ray sources associated with active galaxies and characterized by nonthermal spectra. Such "blazars" are highly variable and are bright radio sources. The radio structure consists of knotty jets moving outward at high velocities. The luminosity in gamma rays can exceed that from other wavelengths by up to two orders of magnitude. The variability of the emission can be fast, less than a week. The density of high energy gammas at the source are sufficient that photon-photon pair production would keep them trapped, unless the gammas are highly beamed, as in a relativistic jet. Thus the hope is that the gamma ray spectrum can yield information on the nature of the jet and of the acceleration processes occurring there. It is thought that the gamma rays may originate from a region of the jet closer to the central engine, than in the case of the radio emission.

A few blazars have been observed producing very high energy gamma rays, up to TeV scales. One, Markarian 421, was measured in the TeV range by the Whipple Observatory, which detects Cerenkov radiation from air showers. It was not seen at GeV energies by EGRET. The high energy flare had a rise time of about two days. One day after the flare commenced this source was seen in the X-ray. Both of these signals differ from typical blazars in their higher energies: most blazars have lower energy gamma and low-energy radiation that does not extend into the x-ray. The interpretation is that blazars accelerate electrons to high energies, which then radiate soft synchrotron radiation and hard gammas by inverse Compton scattering. Markarian 421 is thus exceptional in the energies to which it accelerates electrons, accounting for the higher energy of its x-ray/gamma emission.

Markarian 421, which was first observed in May, 1994, is not unique. The second closest

blazar of this type, Markarian 501 ($z=0.034$), was seen in 1997. It flared to become the brightest TeV source in the sky, outshining the Crab Nebulae by an order of magnitude. The periods of flaring lasted a few days. The elevated activity spanned a period from about March through June. The high energy spectrum (observed by Whipple) was flat from below a TeV to at least 10 TeV. The x-ray cutoff in Markarian 421 is about 1 keV; in Markarian 501 it is above 100 keV. As in 421, it is assumed that this spectrum comes from relativistic acceleration of electrons along a jet closely aligned with our line of sight.

What does this tell us about the electron energies? First, the plasma in the jet is moving towards us, boosting the energy of the emitted gammas, relative to the jet rest frame. The Doppler factor is

$$D = \frac{\sqrt{(1 - v^2/c^2)}}{(1 + z)(1 - v \cos \theta/c)}$$

where θ is the observation angle relative to the jet axis. This is the standard relativistic Doppler shift corrected by the redshift. The observed energy of the gamma rays is

$$E_{max} \sim D\gamma m_e c^2$$

where $\gamma m_e c^2$ is the maximum energy of the electrons in the jet rest frame. The Doppler factor also appears in the calculation of the photon density in the blob, and thus of the blobs opacity to high energy γ s. The argument goes as follows: if Δt_{obs} is the fastest observed TeV gamma ray flare variability, then the radius of the blob emitting the photons must be less than

$$\sim cD\Delta t_{obs}$$

Thus a larger D means a lower photon density. From this one concludes $D \gtrsim 30$. Since the highest energy gammas from Markarian 501 is about 20 TeV, one derives for the maximum energy of electrons in the jet frame

$$\gamma m_e c^2 \sim 0.65 \text{ TeV}$$

Since the maximum electron velocity is now known, one can deduce the magnetic field in the jet required to produce synchrotron radiation with a maximum energy of 200 keV. That yields

$$E_{max} \propto DB\gamma^2 \Rightarrow B \sim 0.7G$$

where B is the field in the jet rest frame. Other aspects of the blazar dynamics - such as the physics responsible for the short timescale of the flares - is less clear.

Another exciting result involving high energy γ s are the gamma ray burst observations of EGRET. While the vast majority of the bursts are seen by BATSE, on the order of 10% of the events produce spectra that extend into EGRET's range of above 30 MeV, typically producing about five counts. The most dramatic event was that of February 17, 1994, in which the high-energy gamma ray emission appeared to extend for an hour or more beyond the sub-MeV emission detected by BATSE. The highest energy event was at 18 GeV and occurred almost an hour after the BATSE observations ended.

These high energy tails place a lot of constraints on gamma ray burst models. Since high energy gammas were also seen early in the burst, there must be high-energy particle acceleration simultaneous to the keV emission. The lack of attenuation of high energy γ s from $\gamma-\gamma$ pair production off lower energy γ s place a particularly strong constraint on the source and on models involving beaming.

Finally, a third interesting source of high energy γ s are both isolated and binary pulsars. Gamma ray emission can be very strong, representing 10% or more of the spin-down energy of some pulsars. There is relatively little consensus on the mechanism or even the precise site of the gamma ray production (neutron star surface? accretion disk? etc?)

Centaurus X-3 is a well-studied high-mass accreting X-ray binary. EGRET measured a

smoothly declining spectrum that extended from 100 MeV to its detection limit. Results have been reported from the Durham Mark 6 gamma ray telescope in the vicinity of a TeV: the flux is consistent with a linear extrapolation of the EGRET flux. Centaurus X-3 contains a 4.8s pulsar in a 2.1 day orbit about an O-type supergiant V779 Centaurus. The pulsar period has been shortening since its discovery almost 30 years ago, which is attributed to spin-up from matter accreting on the neutron star from the more rapidly rotating inner edge of its accretion disk. The EGRET GeV burst observations were pulsed in agreement with the X-ray period. Initial TeV gamma ray observations also indicated pulsation near the pulsar period and localized in But later measurements at high energy indicated unpulsed emission that one would then associated with radiation over an extended volume encompassing the orbit.

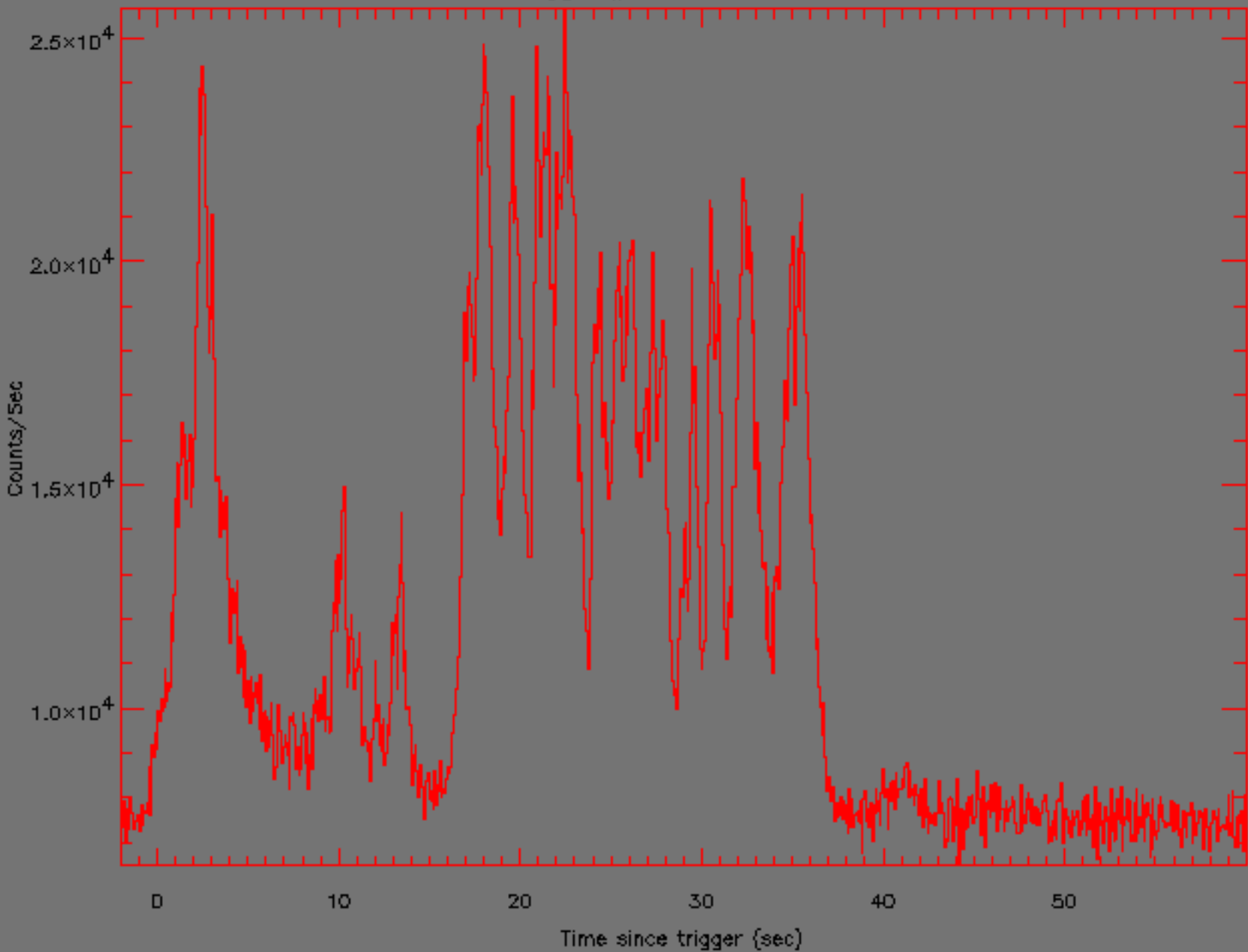
8.7 Gamma ray bursts

Gamma ray burst have been mentioned several times. Gamma ray bursts are short-lived burst lasting from a few milliseconds to several minutes. They are detected roughly once per day, from all directions in the sky. They represent tremendous energy, several hundred times brighter than a typical supernova (were they radiated in 4π). They were originally detected in the 1960s by military satellites monitoring nuclear testing. They are not local, but originate at cosmological distances. In the past few years it has become clear they are associated (at least some of the time) with certain supernovae.

Recently fast-response telescopes - like NASA's High-Energy Transient Explorer or the Japanese Automated Response Telescope - have been able to view the gamma-ray burst area within a couple of minutes of the burst. The "afterglows" have been observed for on the order of an hour to a day after the burst – representing a lot of additional energy.

General ideas exist that gamma ray bursts are associated with fireball phenomena where tremendous energy and high velocities are produced in a region relatively free of baryons –

Trigger #2852 E > 25 keV



to keep the gamma rays from thermalizing. The motion leads to a beaming of the burst, reducing the energy requirements but increasing the frequency of events (many of which are not beamed at earth and thus are not observed).

A specific idea is the hypernova. A massive star's core collapses into a black hole. The black hole's spin or magnetic fields may act like a slingshot, flinging material outward as a beamed blast wave or jet. The gamma rays are created when the blast wave collides with stellar material still inside the star. The gamma rays burst out of the star just in front of the blast wave. Behind the gamma rays, the blast wave pushes the stellar material outward.

The blast wave then sweeps through space, colliding with gas and dust, producing additional radiation – progressing from less energetic gammas, to x-rays, to visible light, and to radio. This forms the afterglow, lasting perhaps up to days.